ISSN 1674-1056
http://cpb.iphy.ac.cn
http://iopscience.iop.org/cpb
中国物理 B
Chinese Physics
中国物理
Chinese Physics B

Influences of substrate temperature on microstructure and corrosion behavior of APS $Ni_{50}Ti_{25}Al_{25}$ inter-metallic coating

Sh Khandanjou, M Ghoranneviss, Sh Saviz, M Reza Afshar
Citation: Chin. Phys. B . 2018, 27(2): 028104. **doi:** 10.1088/1674-1056/27/2/028104

Journal homepage: http://cpb.iphy.ac.cn; http://iopscience.iop.org/cpb

What follows is a list of articles you may be interested in

Segregations and desorptions of Ge atoms in nanocomposite $Si_{1-x}Ge_x$ films during high-temperature annealing

Yu Wang(汪煜), Meng Yang(杨濛), Gang Wang(王刚), Xiao-Xu Wei(魏晓旭), Jun-Zhuan Wang(王军转), Yun Li(李昀), Ze-Wen Zou(左则文), You-Dou Zheng(郑有炓), Yi Shi(施毅)
Chin. Phys. B . 2017, 26(12): 126801. **doi:** 10.1088/1674-1056/26/12/126801

Preparation and characterization of PTFE coating in new polymer quartz piezoelectric crystal sensor for testing liquor products

Gu Yu, Li Qiang
Chin. Phys. B . 2015, 24(7): 078106. **doi:** 10.1088/1674-1056/24/7/078106

Epitaxial growth of $Ge_{1-x}Sn_x$ films with x up to 0.14 grown on Ge (00l) at low temperature

Tao Ping, Huang Lei, Cheng H H, Wang Huan-Hua, Wu Xiao-Shan
Chin. Phys. B . 2014, 23(8): 088112. **doi:** 10.1088/1674-1056/23/8/088112

Formation of $ZnGa_2O_4$ films by multilayer deposition and subsequent thermal annealing

Yan Jin-Liang, Zhao Yin-Nü, Li Chao
Chin. Phys. B . 2014, 23(4): 048105. **doi:** 10.1088/1674-1056/23/4/048105

Molecular-beam epitaxy of topological insulator Bi_2Se_3 (111) and (221) thin films

Xie Mao-Hai, Guo Xin, Xu Zhong-Jie, Ho Wing-Kin
Chin. Phys. B . 2013, 22(6): 068101. **doi:** 10.1088/1674-1056/22/6/068101

Influences of substrate temperature on microstructure and corrosion behavior of APS $Ni_{50}Ti_{25}Al_{25}$ inter-metallic coating

Sh Khandanjou[1], M Ghoranneviss[1], Sh Saviz[1,†], and M Reza Afshar[2]

[1] *Plasma Physics Research Center, Science and Research Branch, Islamic Azad University, Tehran, Iran*
[2] *Department of Materials Engineering, Science and Research Branch, Islamic Azad University, Tehran, Iran*

(Received 25 June 2017; revised manuscript received 23 October 2017; published online 5 January 2018)

In the present investigation, $Ni_{50}Ti_{25}Al_{25}$ (at.%) mechanically alloyed powder is deposited on carbon steel substrate. Before the coating process, the substrate is heated to temperature ranging from room temperature to 400 °C. The microstructure, porosity, microhardness, adhesion strength, and corrosion behavior of the coating are investigated at different substrate temperatures. Results show that coating porosity is lower on high temperature surface. Microhardness and adhesion strength of the deposition layer on the substrate without preheating have lower values than with preheating. The polarization test result shows that corrosion performance of the coating is dependent on micro cracks and porosities and the increasing of substrate temperature can improve the quality of coating and corrosion performance.

Keywords: $Ni_{50}Ti_{25}Al_{25}$ coating, air plasma spray, planetary ball milling, inter-metallic compounds, corrosion resistance

PACS: 81.15.–z, 68.55.–a, 81.70.Bt, 81.65.–b **DOI:** 10.1088/1674-1056/27/2/028104

1. Introduction

Ni-based inter-metallic coatings have good anti-corrosion and anti-erosion properties at high temperatures; this explains why the researchers are so interested in this field.[1–6] Many studies have been conducted on Ni–Ti and Ni–Al inter-metallic coatings that indicate the importance of these coatings and their applications in many industries.[7–9] The Ni–Ti coatings are widely used in shape memory applications[10–12] and Ni–Al coatings show good anti-corrosive properties.[13] In many studies, researchers have evaluated various combinations of Al and Ti in Ni-base coatings to improve the properties of coatings.[14,15] But recently in order to improve the mechanical and corrosion properties of the binary systems, the combination of nickel, titanium and aluminum has been presented.[16–18] According to good corrosion resistance of each of these materials in corrosive environments, the coatings by the combination of these materials can be utilized in various industries including, oil and gas, aerospace, automobile, etc. Therefore, different techniques for producing these coatings have been presented. One of the best methods is atmospheric plasma spraying (APS). In this method, there is no limit to the size of piece and the APS technique can deposit many different kinds of materials such as metals, ceramics, polymers cermets and high melting point materials.[19] Many parameters influence the quality of plasma spray coatings such as spray distance, plasma power, gas flow rate, powder feeding rate etc. However, in recent years, just one study has been conducted on the effect of plasma spray power on Ni–Ti–Al coating properties.[20] On the other hand, apart from the parameters mentioned above, the substrate preheating temperature is one of the most important parameters that can affect the mechanical and corrosion properties of coating.[21–23] To our knowledge, the effects of substrate temperature on morphology, mechanical properties and electrochemical polarization properties of plasma sprayed $Ni_{50}Ti_{25}Al_{25}$ coating have not been reported so far. Therefore, the aim of the present study is to evaluate the effects of substrate preheating on microstructure, micro hardness, adhesion strength and corrosion behavior of $Ni_{50}Ti_{25}Al_{25}$ intermetallic coatings in detail.

2. Experimental procedure

2.1. Powder feedstock materials preparation

In this article $Ni_{50}Ti_{25}Al_{25}$ (at.%) powders, were prepared by mechanical alloying method by using a planetary ball mill (home-made) for plasma spraying process. Figure 1 shows the morphology of initial powders and Table 1 gives the characteristic of feedstock. In order to protect powders from oxidizing, the mechanically alloying process was conducted in an Ar atmosphere. Furthermore to protect feedstock materials against aggregation 3-wt% stearic acid should be added before putting the materials in a planetary ball mill. The planetary milling system was composed of a stainless steel container and 10-mm diameter steel balls. Ball-to-powder weight ratio (BRR) was 10:1 and the impeller was rotated at a speed of about 340 rpm. The $Ni_{50}Ti_{25}Al_{25}$ (at.%) powders were prepared at different mechanically alloying times to the most suitable powder was selected for plasma spray process.

†Corresponding author. E-mail: azarabadegan@gmail.com

© 2018 Chinese Physical Society and IOP Publishing Ltd

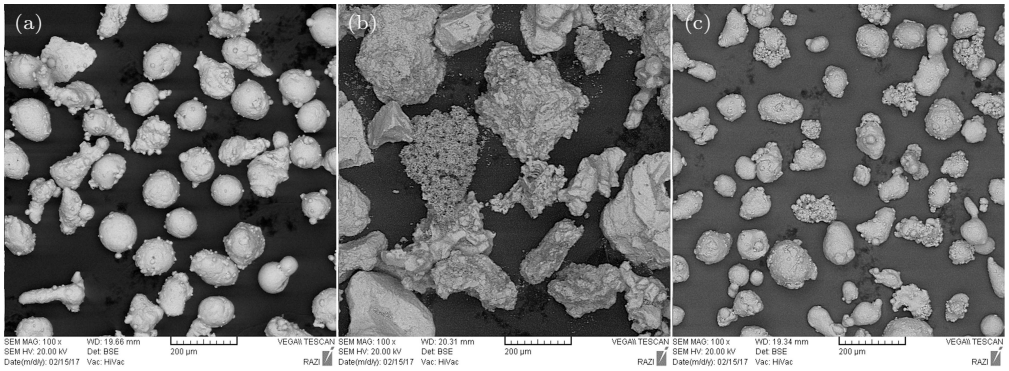


Fig. 1. SEM images of initial powders: (a) Nickel, (b) titanium, and (c) aluminum.

Table 1. Feedstock material specifications.

Feedstock powder	Size/μm	Purity
Nickel	50–100	99 %
Titanium	100–300	99%
Aluminum	50–100	99%

2.2. Thermal plasma spraying system

In the present study, the plasma torch system that was used to deposit $Ni_{50}Ti_{25}Al_{25}$ (at.%) coating was developed in the Plasma Physics Research Centre. Figure 2 shows the schematic diagram of the plasma torch system. Argon gas was used to produce plasma and powder feed gas. In this research, a low carbon steel sheet (0.08% C, 0.017% Si, 0.017% P, 0.423% Mn, 0.025% Ni, 0.003% S, 0.006% Cr, balance Fe), was cut and used as substrate. To increase adhesion between the substrate and coating, all steel substrates were pre-treated by grit-blasting with aluminium oxide (Al_2O_3) particles. In all of the experiments, the powder was injected into the plasma jet vertically. In order to reduce the internal stress in the coating, all the samples were cooled to room temperature. The main parameters of the plasma spray system used in this study are presented in Table 2.

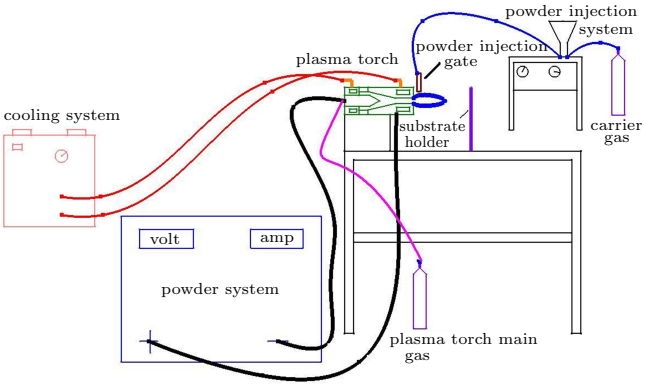


Fig. 2. (color online) Schematic diagram of plasma torch system.

Table 2. Technical specification of APS system.

Parameters	Unit
Working gas	argon
Arc current/A	500
Arc voltage/V	50
Stand-off distance/mm	120
Powder feeding rate/(g/min)	20
Plasma gas flow rate/(L/min)	40

2.3. Feedstock materials and coating characterizations evaluation

Phase compositions of powders and coatings are analyzed by x-ray diffraction (XRD, STADI-MP) with Cu Kα radiation ($\lambda = 1.54056$ Å). To evaluate the surface properties of the deposition layer, a scanning electron microscope (SEM, VEGAII TESCAN) equipped with energy dispersive x-ray analysis (EDX) was utilized and the porosity percentage of coating was calculated by using image analysis software (ImageJ).

2.4. Mechanical properties measurement

In this research, Vickers microhardness testing device, (BUEHLER) was used to measure the microhardness values of coatings, according to the ISO/IEC17025 standard. Applied force was 500 grf for 10 s–15 s. For each sample, hardness test was performed five times on the polished cross section surfaces and the average of the results was recorded. Also, the microhardness values of samples in the substrate-coating interface were evaluated.

In addition, the adhesion strengths of coatings are measured by pull-off device (DEFELESCO) at three different points and their average was reported as the adhesion strength of each coating.

2.5. Tafel polarization test

In this research, the electrochemical polarization test was used to investigate the corrosion behaviour of the coating. Test results are recorded at room temperature using an electro-chemical apparatus consisting of a platinum coil as the counter-electrode and calomel reference electrode in 3.5 wt% sodium chloride solution (NaCl), using an EG & G potentiostat (model 273 A). The test was started after 1-hour immersion with 1-mV/s scan rate. The corrosion potentials (E_{corr})

and corrosion current density (i_{corr}) were obtained with the aid of 'Cview' software.

3. Results and discussion

3.1. Microstructure analyses of $Ni_{50}Ti_{25}Al_{25}$ powders at different times of mechanically alloying

The quality of plasma sprayed coating is influenced by the size and structure of the feedstock powder material.[24] Figure 3 shows the XRD patterns of powder particles at different times of planetary milling. As the figure shows, after 16 h milling distinguishable phases are pure nickel, titanium and aluminum and no new inter-metallic phases are formed. A comparison among the XRD patterns at different milling times shows that the intensity of initial material peak decreases by increasing the milling time, slightly. This is because of reducing the crystallite size and increasing the dislocations caused by the internal strain which increases during mechanically alloying.[25]

The SEM of feedstock particles after planetary milling is presented in Fig. 4. The morphologies of powders indicate that the lamellar structures are formed in all of the samples. When the lamellar structure exists in the structure, the formation of inter-metallic compounds increases during thermal plasma spraying due to the provision of large interfaces for exothermic reaction.[26] When the mechanically alloying time is increased, more homogenous lamellar structure is produced. But, the particle size becomes very small and the small nano-particles move from the powder feeder device to plasma torch nozzle with difficulty. Furthermore, nano-particles more or less evaporate in the thermal plasma jet.[27] So, in this study, $Ni_{50}Ti_{25}Al_{25}$ particles that are milled for 2 h are used. These particle sizes are between 20 μm and 70 μm.

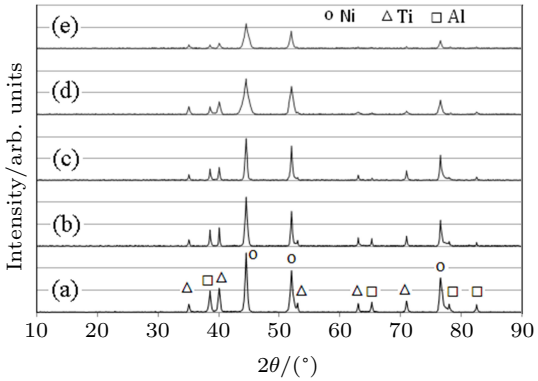


Fig. 3. XRD pattern of feedstock powder particles at milling times of (a) 2 h, (b) 4 h, (c) 8 h, and (d) 16 h.

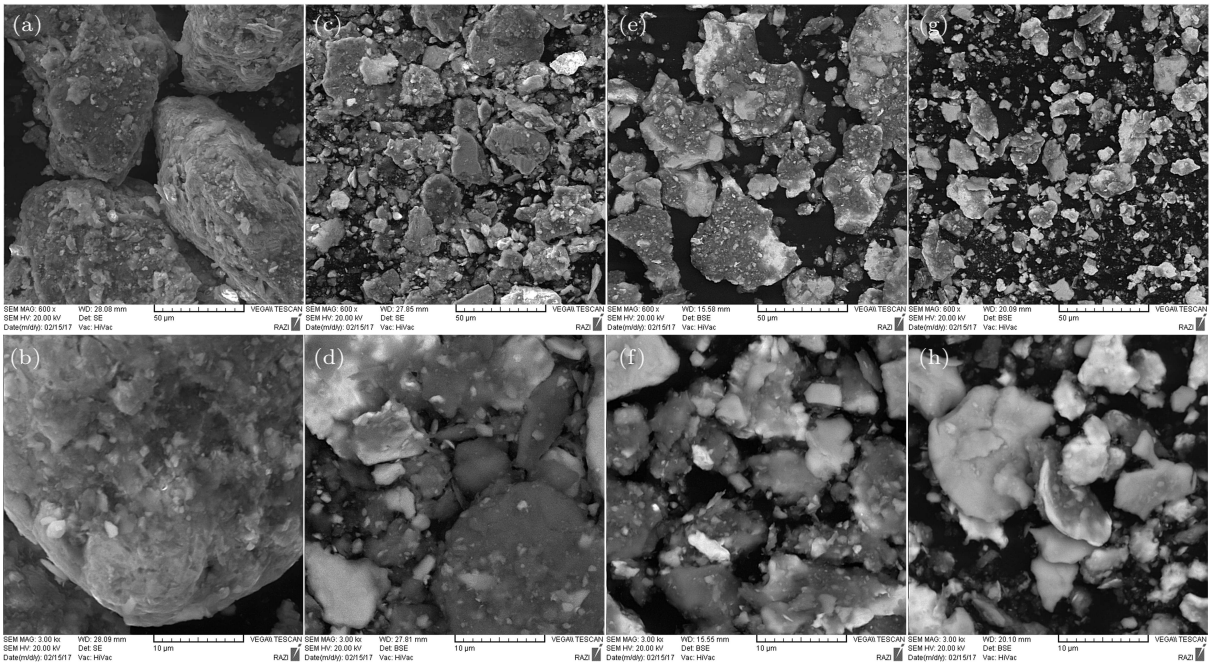


Fig. 4. SEM images of powder particles at milling times of ((a), (b)) 2 h, ((c), (d)) 4 h, ((e), (f)) 8 h, and ((g), (h)) 16 h.

3.2. Microstructure analyses of APS $Ni_{50}Ti_{25}Al_{25}$ coatings

Figure 5 presents the XRD patterns of coatings at substrate temperature from room temperature to 400 °C. The formation of an inter-metallic compound occurs at a suitable time and heating. With increasing substrate temperature, the probability of forming inter-metallic phases is higher. It shows the formation of different inter-metallic compounds such as $Ni_3(Ti,Al)$ and Ni_2TiAl phases and also Ni and TiO, during spraying. This phenomenon is not unexpected. These phases can also be seen in other research.[20,28] The $Ni_3(Ti, Al)$ phase causes anti-corrosion properties at high temperature.[29] In addition, the XRD pattern shows that at high substrate temperature, the intensity in the direction of the Ni peak is lower and the intensity in the direction of the $Ni_3(Ti, Al)$ peak is higher than others.

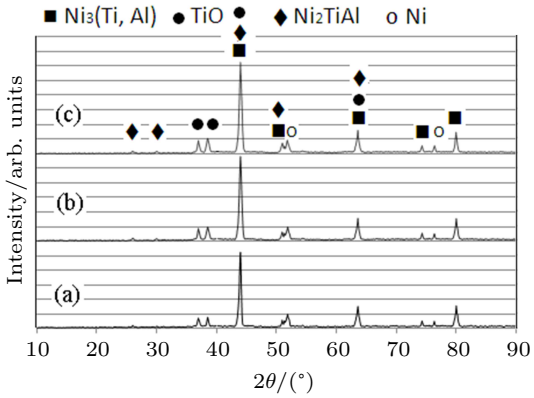


Fig. 5. XRD patterns of coatings at substrate temperatures of (a) room temperature, (b) 200 °C, and (c) 400 °C.

Figure 6 shows the SEM images of the cross section of deposition layers at different substrate temperatures. As can be seen in the figure, the Ni–Ti–Al coating without preheating contains some pores and voids. With the increase of the temperature of substrate, coatings each exhibit a uniform structure by minimizing the amount of porosity in the cross-sections of coatings. The porosity percentage of the cross-section of coating is calculated by ImageJ software. This calculation is repeated five times and the averages are about 8.4% for coating without preheating and 3.7% and 1.6% for coatings with preheating at 200 °C and 400 °C substrate temperature, respectively. When the surface is preheated prior to the coating, the deposition layer is more uniform with less porosity. This is because when the temperature of the substrate increases, the wettability increases. This provides better mechanical anchorage between the particles and substrate but in the surface without preheating, the heat of the particles is transferred to a cool substrate and the required wetting effect is not provided.[30] Therefore, the porosity of coating without preheating is more than with preheating.

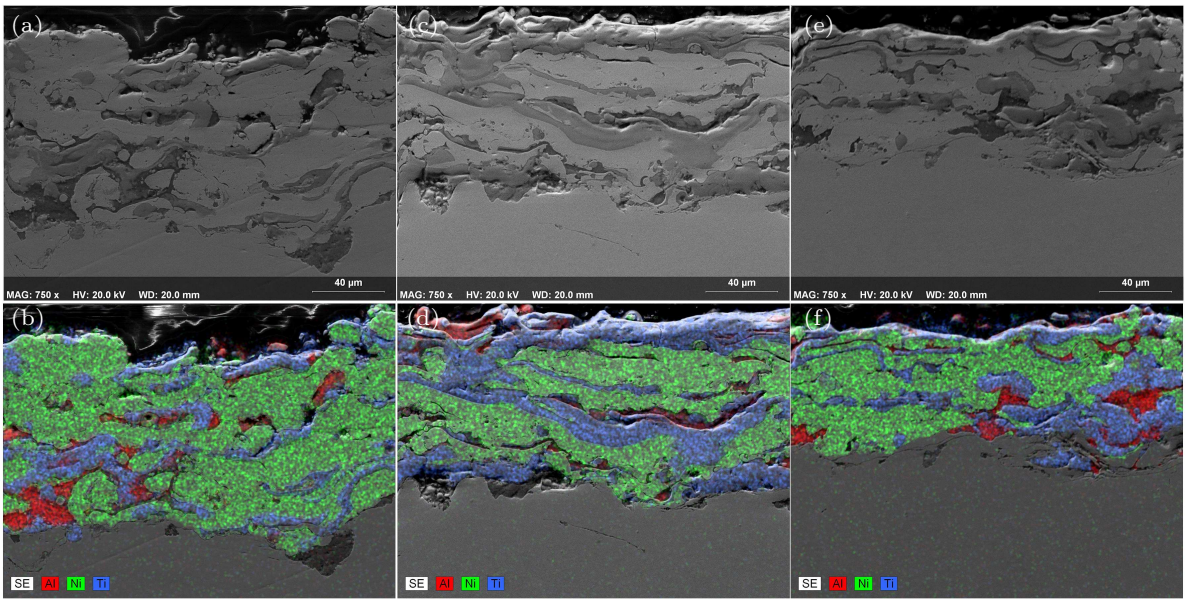


Fig. 6. (color online) SEM cross section images of deposition layers at substrate temperatures of ((a), (b)) room temperature, ((c), (d)) 200 °C, and ((e), (f)) 400 °C.

3.3. Microhardness and adhesion strength measurement

One of the important mechanical properties of coating is microhardness. In all the coatings, inter-metallic phase greatly affects the microhardness of coating. In this research, it is found that with substrate temperature increasing from 200 °C to 400 °C, the microhardness value increases from 304 HV to 444 HV and the microhardness of coating without preheating is less, about 283 HV. This is due to higher flattening, less porosity and higher number of inter-metallic phases in the coatings with high substrate temperature.

Another important mechanical property of the coating is adhesion strength. As mentioned previously, when the temperature of the substrate increases, the wettability increases and this provides an excellent weld between the particles and substrate surface, thereby resulting in better adhesion between impacting particles and the substrate. So, with substrate temperature changing from room temperature to 200 °C and 400 °C, the adhesion strength increases from 13.7 MPa to 18.5 MPa and 20.4 MPa, respectively. Studies show that as the substrate temperature increases, the coated particles become disk shaped. In contrast, at low substrate temperature, the coated particles are irregular. Disk splats provide better substrate-coating adhesion strengths than irregular splats.[23]

In this study, for better observing the adhesion between coating and substrate, interfacial indentation test is used. A square-based pyramidal-shaped diamond indenter is used at the interface between the substrate and surface. The load of the indenter is similar to the microhardness test for coating layer (500 grf). This experiment also shows the APS coating with 400 °C preheating temperature, and records the best adhesion. Figure 7 shows that there is no crack at the interface of the coating with 400 °C preheating temperature, after the interfacial indentation test.

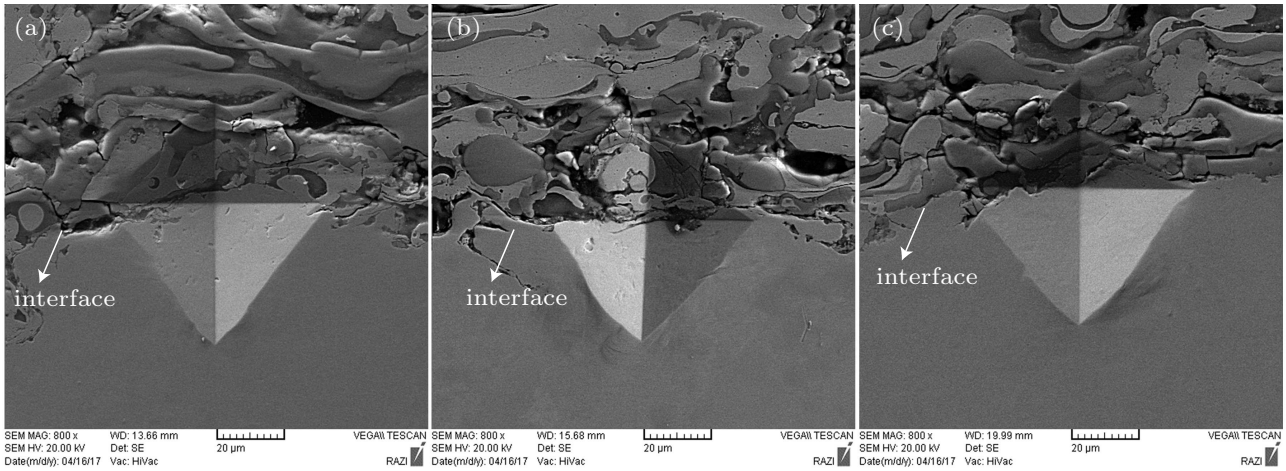


Fig. 7. Vickers test traces in the coating-substrate interface at substrate temperatures of (a) room temperature, (b) 200 °C, and (c) 400 °C.

3.4. Corrosion behavior of coating

The electrochemical polarization behaviors of the coatings and substrate are presented in Fig. 8. Polarization curves show that polarized coatings have higher corrosion potentials and lower current densities than carbon steel substrate. This means that substrate corrosion occurs earlier than coating. It is clear from Table 3 that the current density of coating decreases by increasing the substrate temperature. Therefore, the corrosion resistance increases due to the increase in preheating temperature, low porosity, and better coating-substrate adhesion. When the coating has a high number of micro cracks and pores, the corrosion rate of coating increases, because the electrolyte is driven to the substrate and prevention of a homogeneous passive layer form forming.[28]

Table 3. Technical specification of APS system.

Substrate temperature/°C	E_{Corr}/V	I_{Corr}/(μA·cm^{-2})
Room temperature	−0.621	6.048
200	−0.599	5.695
400	−0.521	5.320

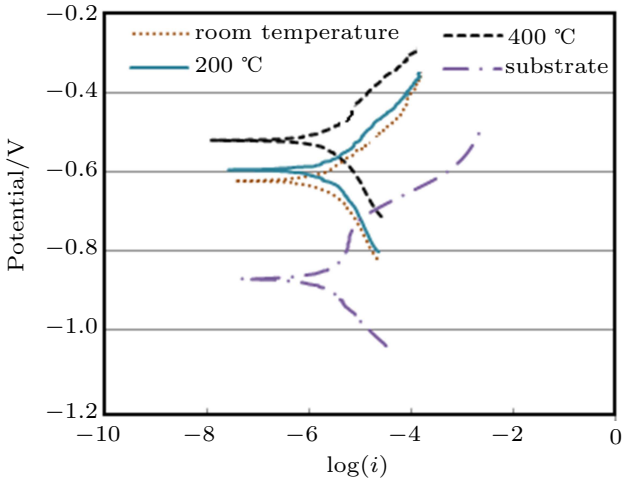


Fig. 8. (color online) Tafel polarization plots of coating and carbon steel substrate.

4. Conclusions

(i) The XRD results show that in the Ni–Ti–Al powders mechanically alloyed for 16 h, no inter-metallic phase is formed. But APS coating by mechanically alloying powder for 2 h, involves inter-metallic phases such as Ni_3(Ti, Al), Ni_2TiAl, and TiO.

(ii) With increasing the temperature of substrate, coating exhibits a homogeneous structure with low porosity in the cross-section of coating due to the wettability increasing and better mechanical anchorage of particles.

(iii) Microhardness and adhesion strength evaluation show that the higher melting fraction of particles causes the less porous coating to form. So, the coating with 400 °C substrate temperature presents the best mechanical properties because of disk shape of coated particles. Disk splats provide better contact and better substrate-coating adhesion strength.

(iv) Electrochemical polarization analysis shows higher corrosion resistance of $Ni_{50}Ti_{25}Al_{25}$ coating by increasing the substrate preheating temperature due to low porosity and better coating–substrate adhesion without micro cracks.

References

[1] Hsieh S F and Wu S K 1997 *J. Mater. Sci.* **32** 989
[2] Cinca N, Lima C R C and Gulimany J M 2013 *J. Mater. Res. Technol.* **2** 75
[3] Liu K T and Duh J G 2008 *Surf. Coating Technol.* **202** 2737
[4] Zadorozhnyy V, Kaloshkin S, Tcherdyntsev V, Gorshenkov M, Komissarov A and Zadorozhnyy M 2014 *J. Alloys Compd.* **586** 373
[5] Meng L J, Li Y, Zhao X Q, Xu J and Xu H B 2007 *Intermetallics* **15** 814
[6] Yoruk G and Ozdemir O 2012 *Intermetallics* **25** 60
[7] Frommeyer G and Rabibauer R 2008 *Mater. Technol.* **79** 507
[8] Noebe R D, Bowman R R and Nathal M V 1996 *Physical Metallurgy and Processing of Intermetallic Compounds* 212
[9] Hyjek P, Sulina I and Malczewski P 2015 *Metallurgy and Foundary Engineering* **41** 29
[10] Surbled P, Clerc C, Pioufle B L, Ataka M and Fujita H 2001 *Thin Solid Films* **401** 52
[11] Morgan N B 2004 *Mater. Sci. Eng. A* **378** 16

[12] Lehnert T, Grimmor H, Boni P, Orisberger M H and Gotthardt G 2000 *Acta Mater.* **48** 4065
[13] Javadi M M, Edris H and Salehi M 2011 *J. Mater. Sci. Technol.* **27** 816
[14] Hou G, An Y, Zhao X, Zhao H and Chen J 2016 *Tribology International* **94** 138
[15] Guanhong S, Xiaodong H, Jiuxing J and Tue S 2011 *Appl. Surface Sci.* **257** 7864
[16] Chen T and Wu J 2016 *Appl. Sci.* **6** 70
[17] Sheng L, Zhang W, Gue J, Yang F, Liang Y and Ye H 2010 *Intermetallics* **18** 740
[18] Shi J, Cao Z H, Wei M Z, Pan G J, Xu L J and Meng X K 2015 *Mater. Sci. Eng. A* **623** 104
[19] Lampe T, Eisenberg S and Cabeo E R 2003 *Surf. Coatings Technol.* **174** 1
[20] Sichani H R, Salehi M, Edriss H and Farani M T 2017 *Surf. Coatings Technol.* **309** 959
[21] Tsipas and Alexandra S 2011 *J. Eur. Ceram. Soc.* **31** 2923
[22] Tang D 2015 *IOP Conf. Series: Mater. Sci. Eng. A* **87** 012097
[23] Pershin V, Lufitha M, Chandra S and Mostaghimi J 2003 *J. Thermal Spray Technology* **12** 370
[24] Kumar S, Selvarajan V, Padmanabhan P V A and Sreekumar K P 2008 *Mater. Sci. Eng. A* **486** 287
[25] Karolus M and Panek J 2016 *J. Alloys Compd.* **658** 709
[26] Movahedi B and Jazi H S 2012 *Adv. Plasma Spray Applications* 189
[27] Wan Y P, Fincke J R, Sampath S, Prased V and Herman H 2002 *Int. J. Heat Mass Transfer* **45** 1007
[28] Ojo O A, Richards N L and Chaturvedi M C 2004 *J. Mater. Sci.* **39** 7401
[29] Guilemany J M, Cinca N, Dosta S and Benedetti A V 2009 *Corrosion Science* **51** 171
[30] Paredes R S C, Amico S C and d'Oliveira A S C M 2006 *Surf. Coatings Technol.* **200** 3049